


RESEARCH ARTICLE

Structural and functional asymmetry of medial temporal subregions in unilateral temporal lobe epilepsy: A 7T MRI study

Preya Shah^{1,2}  | Danielle S. Bassett^{1,3,4,5}  | Laura E.M. Wisse^{6,7} | John A. Detre^{4,7,8} | Joel M. Stein⁷ | Paul A. Yushkevich^{6,7} | Russell T. Shinohara⁹ | Mark A. Elliott⁷ | Sandhitsu R. Das^{4,6†} | Kathryn A. Davis^{2,4†} 

¹Department of Bioengineering, School of Engineering and Applied Science, University of Pennsylvania, Philadelphia, Pennsylvania

²Center for Neuroengineering and Therapeutics, University of Pennsylvania, Philadelphia, Pennsylvania

³Department of Electrical and Systems Engineering, School of Engineering and Applied Science, University of Pennsylvania, Philadelphia, Pennsylvania

⁴Department of Neurology, Perelman School of Medicine, University of Pennsylvania, Philadelphia, Pennsylvania

⁵Department of Physics and Astronomy, College of Arts and Sciences, University of Pennsylvania, Philadelphia, Pennsylvania

⁶Penn Image Computing and Science Laboratory, University of Pennsylvania, Philadelphia, Pennsylvania

⁷Department of Radiology, Perelman School of Medicine, University of Pennsylvania, Philadelphia, Pennsylvania

⁸Center for Functional Neuroimaging, University of Pennsylvania, Philadelphia, Pennsylvania

⁹Department of Biostatistics, Epidemiology, and Informatics, Perelman School of Medicine, University of Pennsylvania, Philadelphia, Pennsylvania

Correspondence

Preya Shah, University of Pennsylvania, Philadelphia, PA 19104.

Email: preya@pennmedicine.upenn.edu

Funding information

Mirowski Family Foundation; TAPITMAT-TBIC, Grant/Award Number: UL1TR001878; Thornton Foundation; Mirowski Family Foundation; Center for Biomedical Image Computing and Analytics Seed Award; Transdisciplinary Awards Program in Translational Medicine and Therapeutics-Translational Biomedical Imaging Core (TAPITMAT-TBIC), Grant/Award Number: UL1TR001878; National Institutes of Health, Grant/Award Numbers: R01EB017255, R01MH112847, R01NS085211, 1R01NS099348-02, K23-NS073801-01, R03-EB16923-01A1, T32-EB009384

Abstract

Mesial temporal lobe epilepsy (TLE) is a common neurological disorder affecting the hippocampus and surrounding medial temporal lobe (MTL). Although prior studies have analyzed whole-brain network distortions in TLE patients, the functional network architecture of the MTL at the subregion level has not been examined. In this study, we utilized high-resolution 7T T2-weighted magnetic resonance imaging (MRI) and resting-state BOLD-fMRI to characterize volumetric asymmetry and functional network asymmetry of MTL subregions in unilateral medically refractory TLE patients and healthy controls. We subdivided the TLE group into mesial temporal sclerosis patients (TLE-MTS) and MRI-negative nonlesional patients (TLE-NL). Using an automated multi-atlas segmentation pipeline, we delineated 10 MTL subregions per hemisphere for each subject. We found significantly different patterns of volumetric asymmetry between the two groups, with TLE-MTS exhibiting volumetric asymmetry corresponding to decreased volumes ipsilaterally in all hippocampal subfields, and TLE-NL exhibiting no significant volumetric asymmetries other than a mild decrease in whole-hippocampal volume ipsilaterally. We also found significantly different patterns of functional network asymmetry in the CA1 subfield and whole hippocampus, with TLE-NL patients exhibiting asymmetry corresponding to increased connectivity ipsilaterally and TLE-MTS patients exhibiting asymmetry corresponding to decreased connectivity ipsilaterally. Our findings provide initial evidence that functional neuroimaging-based network properties within the MTL can distinguish between TLE subtypes. High-resolution MRI has potential to improve localization of underlying brain network disruptions in TLE patients who are candidates for surgical resection.

KEYWORDS

7 tesla MRI, medial temporal lobe, mesial temporal sclerosis, network neuroscience, resting-state fMRI, temporal lobe epilepsy

†S. R. Das and K. A. Davis contributed equally to this work.

1 | INTRODUCTION

Mesial temporal lobe epilepsy (TLE) is the most common type of localization-related epilepsy, affecting approximately one in 1,000 people worldwide (Engel, 2001; Kwan, Schachter, & Brodie, 2011; Wieser, 2004). Approximately 30% of TLE patients do not respond to medical therapy and are candidates for surgical removal of the seizure-generating area (Engel, 1996). Accurate seizure localization prior to surgery is crucial in order to maximize chances of seizure freedom and minimize post-surgical cognitive deficits. While approximately two-thirds of TLE patients have mesial temporal sclerosis (MTS) identified on structural MRI (TLE-MTS), the remaining one-third have normal-appearing ("nonlesional") clinical MRI scans (TLE-NL). Lateralization and localization of seizure onset zone in these patients can be difficult, since other neuroimaging and electrophysiology-based tests are often inconclusive, precluding surgical resection. In nonlesional patients who do undergo surgery following invasive localization procedures such as intracranial EEG, post-surgical outcomes are still substantially worse than in patients with well-defined lesions on MRI (Siegel et al., 2001; Téllez-Zenteno, Ronquillo, Moien-Afshari, & Wiebe, 2010). Thus, there remains a pressing clinical need to establish noninvasive neuroimaging biomarkers for nonlesional TLE. Furthermore, with the recent emergence of highly targeted therapeutic options such as laser ablation (Willie et al., 2014) and neurostimulation (Fisher & Velasco, 2014), precise localization of the seizure onset zone will become increasingly valuable for guiding therapy.

It has become widely accepted that the pathophysiology of localization-related epilepsy extends beyond focal lesions to alter the properties of brain networks (Bernhardt, Hong, Bernasconi, & Bernasconi, 2013; Chu et al., 2012; Khambhati, Davis, Lucas, Litt, & Bassett, 2016). As a result, researchers have begun to employ graph theoretical methods to characterize network aberrations in neuroimaging data from TLE patients (Chiang & Haneef, 2014; Haneef & Chiang, 2014). Many of these studies focus only on TLE-MTS (Liao et al., 2010; Pereira et al., 2010) or consider TLE as a single entity without distinguishing between TLE-MTS and TLE-NL groups (Barron et al., 2015; Bettus et al., 2009; Haneef, Lenartowicz, Yeh, Engel, & Stern, 2014; He, Doucet, Sperling, Sharan, & Tracy, 2015; James, Tripathi, Ojemann, Gross, & Drane, 2013; Morgan, Sonmez Turk, Gore, & Abou-Khalil, 2012; Pittau, Grova, Moeller, Dubeau, & Gotman, 2012). However, there is growing evidence that TLE-MTS and TLE-NL may be distinct disorders with distinct underlying pathophysiology and with different network manifestations (Bernhardt et al., 2016a; Liu, Concha, Lebel, Beaulieu, & Gross, 2012; Muhlhofer, Tan, Mueller, & Knowlton, 2017; Reyes et al., 2016; Vaughan, Rayner, Tailby, & Jackson, 2016). These findings suggest that the TLE-MTS and TLE-NL subtypes should be studied separately, to better understand their differences and to promote the discovery of biomarkers specific to TLE-NL.

Most prior work using neuroimaging methods to examine changes in network topology in TLE have focused on whole-brain networks. However, findings from a range of investigative approaches provide initial evidence that network distortions within the MTL itself play a fundamental role in TLE. For example, rodent models of TLE reveal aberrant mossy fiber connections from the granule cell layer to the

stratum moleculare of the dentate gyrus (DG); according to the recurrent excitation hypothesis, the resulting DG hyperexcitability may cause seizures (Sharma et al., 2007). Another example is that histopathology of resected tissue in TLE-MTS patients reveals heterogeneous patterns of atrophy and astrogliosis in the hippocampus and surrounding medial temporal regions (Sharma et al., 2007; Wieser, 2004). From a clinical management standpoint, the extent of resection of various MTL subregions is directly related to seizure control (Bonilha, Martz, Glazier, & Edwards, 2012). In fact, 20% of TLE patients with hippocampal resection still experience seizures originating from remaining MTL structures (Wennberg, Arruda, Quesney, & Olivier, 2002). These findings suggest that the entire MTL subregional network may be implicated in seizure activity, and that understanding this network could improve diagnosis and treatment.

In this study, we used 7 Tesla (7T) MRI to probe fine-grained structure and function within the MTL. Compared to standard clinical MRI, 7T MRI can produce higher resolution images with higher signal-to-noise and contrast-to-noise ratios, facilitating visualization and segmentation of small brain structures with exquisite anatomical detail (Balchandani & Naidich, 2015; van der Kolk, Hendrikse, Zwanenburg, Visser, & Luijten, 2013). Moreover, since the first 7T MRI scanner was approved by the U.S. Food and Drug Administration in late 2017, there is a need to develop tools maximizing the clinical utility of 7T data as they become more readily available. Building on our previous analyses of intra-MTL subregional connectivity in healthy adults (Shah et al., 2018), we employed an automated multi-atlas pipeline on sub-millimeter 7T T2-weighted MRI to segment MTL subregions in TLE patients and healthy controls. In addition to subject-specific subregional volumetric analyses, we applied graph theoretical methods to 7T resting-state BOLD-fMRI data to characterize subject-specific functional MTL subregional networks. We focused on asymmetry-based metrics, as structural and functional asymmetry indices have previously been used to aid in seizure lateralization (Cook, Fish, Shorvon, Straughan, & Stevens, 1992; Davis et al., 2015; Goffin et al., 2010; Jokeit, Okujava, & Woermann, 2001; Pereira et al., 2010; Ver Hoef et al., 2013; Ver Hoef, Williams, Kennedy, Szaflarski, & Knowlton, 2013), and are robust to confounds such as age and gender (Farid et al., 2012; Li, Ga, Huo, Li, & Gao, 2007). We hypothesized that asymmetry-based metrics would reveal distinct patterns of abnormalities in the TLE-NL and TLE-MTS patients. Our preliminary findings provide insight into MTL functional connectivity in TLE, particularly in cases in which standard clinical MRI is unremarkable.

2 | METHODS

2.1 | Subjects

We recruited 29 medically refractory patients with suspected TLE undergoing pre-surgical evaluation. To minimize heterogeneity in this diverse patient population, we excluded subjects with the following characteristics: neocortical rather than mesial temporal onset, dual pathology, extra-temporal lesions, bilateral disease or ambiguous laterality, neoplasms, and other neurological co-morbidities. Seizure laterality, mesial temporal origin, and lesional status were determined

via a combination of MRI and positron emission tomography (PET) imaging, scalp EEG, intracranial EEG, seizure semiology, and epileptologists' clinical notes, and confirmed by an epileptologist for this study (author K.D.). Our final data set consisted of 13 patients with unilateral drug-resistant TLE, including nine TLE-NL and four TLE-MTS (Table 1), along with 24 healthy control subjects (Shah et al., 2018). All studies were conducted under an approved Institutional Review Board protocol of the University of Pennsylvania.

2.2 | Image acquisition

Whole-brain images were acquired using a 7T Siemens whole-body MRI scanner with a 32-channel phased-array head coil (Nova Medical, Wilmington, MA, USA). For all subjects, we obtained $0.4 \times 0.4 \times 1.0 \text{ mm}^3$ MTL-tailored 7T T2-weighted structural variable-flip angle turbo spin-echo MRI ($0.4 \times 0.4 \text{ mm}$ in plane resolution, 1 mm slice thickness, 224 coronal slices, TR = 3,000 ms, TE = 388 ms, 6.16 ms echo spacing) with oblique coronal slices oriented perpendicular to the long axis of the hippocampus and $0.8 \times 0.8 \times 0.8 \text{ mm}^3$ T1-weighted MPRAGE (176 axial slices, TR = 2,800 ms, TE = 4.4 ms, TI = 1,500 ms, flip angle = 7°). We also obtained 2 mm^3 isotropic resting-state BOLD-fMRI using a multiband, gradient-echo echoplanar (EPI) sequence (64 axial slices, TR = 1 s; TE = 23.6 ms, MB factor = 4,420 volumes; 7 min) and a B0 field-map sequence (TR1 = 1 s, TR2 = 100 ms, TE1 = 3.24 ms, TE2 = 5.37 ms).

2.3 | MTL segmentation

To generate MTL segmentations for our data set, we utilized a multi-atlas automated segmentation pipeline derived from the automated segmentation of hippocampal subfields algorithm (Yushkevich et al., 2015) as described and validated in our previous work (Shah et al., 2018). The atlas data set included structural MRI acquired with the protocol described in Section 2.2, and manual expert segmentations of 10 subregions per hemisphere as follows: hippocampal subfields (CA1, CA2, CA3, and DG), hippocampal tail, subiculum, and cortical

regions of the parahippocampal gyrus (entorhinal cortex, parahippocampal cortex, and perirhinal cortex divided into BA35 and BA36) (Figure 1). The hippocampal tail was defined as the most posterior aspect of the hippocampus in which individual subfields could not be discriminated; given the heterogeneity of this region across subjects in terms of size and composition, we excluded it from statistical analyses. We assessed all subjects' images and automated segmentations via rigorous visual inspection to ensure segmentation quality (by authors P.S., L.W.). Representative segmentations from three subjects—one healthy control, one TLE-NL patient, and one TLE-MTS patient—are shown in Figure 2. As illustrated, we observed grossly normal MTL architecture in healthy controls and TLE-NL patients including clearly visible hippocampal digitations (Henry et al., 2011; Oppenheim et al., 1998), and distortion of hippocampal architecture in TLE-MTS.

2.4 | MTL volumetric asymmetry from structural MRI

For TLE-MTS and TLE-NL, we computed volumetric asymmetry indices for each MTL subregion. We also computed an asymmetry index for the hippocampus proper (CA1 + CA2 + CA3 + DG) to facilitate comparison of our findings to prior literature on whole-hippocampal volumetry in TLE-MTS, and since this is the region of interest in the ILAE classification scheme for TLE-MTS (Blümcke et al., 2013). Volumetric asymmetry indices were defined as $[(\text{Contralateral} - \text{Ipsilateral}) / (\text{Contralateral} + \text{Ipsilateral})]$. To account for the presence of inter-hemispheric asymmetries in healthy controls, these indices were subsequently normalized via a z-score transformation with respect to the corresponding distribution of asymmetries in healthy controls (Bernhardt et al., 2016).

2.5 | MTL functional network asymmetry

We describe our preprocessing pipeline for the resting-state BOLD-fMRI data in detail in our previous work (Shah et al., 2018). Briefly, we

TABLE 1 Demographic and clinical information for TLE patients included in this study

Laterality	Lesional status	Gender	Age (years)	Age at onset (years)	Drug trials
Right	MTS	F	41	5	OXC, PB, PHT, TPX, LTG
Right	MTS	F	55	13	CBZ, GBP, LEV, TPX
Left	NL	M	48	5	GBP, LTG, LEV, PB, PHT, PRE, ZNS
Left	MTS	F	61	1	CBZ, LTG, LCM, LEV, PB, PHT, PRM, TPM, ZNS
Left	NL	F	47	41	CBZ, CLB, CNZ, LTG, LCS, LEV, OXC, PHT, PRE, TPX, ZNS
Left	MTS	F	47	Unknown	CLB, GBP, LCM, LEV, OXC, PB, PHT, TIG
Left	NL	F	46	0	PB, OXC, LCM, LTG, LEV, TPX, ZNS
Left	NL	F	56	25	LEV, OXC, LTG, TPX, ZNS, LCM
Left	NL	M	39	36	LEV, LTG, LZP, ZNS
Right	NL	M	36	5	PB, CBZ, VPA, CZP, LTG, LEV
Left	NL	F	32	29	LTG, TPX, ZNS, LEV, OXC
Left	NL	F	37	15	GBP, TPX, LEV, LCM
Left	NL	F	45	24	LTG, ZNS

Legend: VPA = valproic acid, ZNS = zonisamide, OXC = oxcarbazepine, CBZ = carbamazepine, CLB = clonazepam, CZP = clobazepam, LTG = lamotrigine, TPX = topiramate, LEV = levetiracetam, GBP = gabapentin, PB = phenobarbital, PHT = phenytoin, LZP = lorazepam, LCM = lacosamide, PRE = pregabalin.

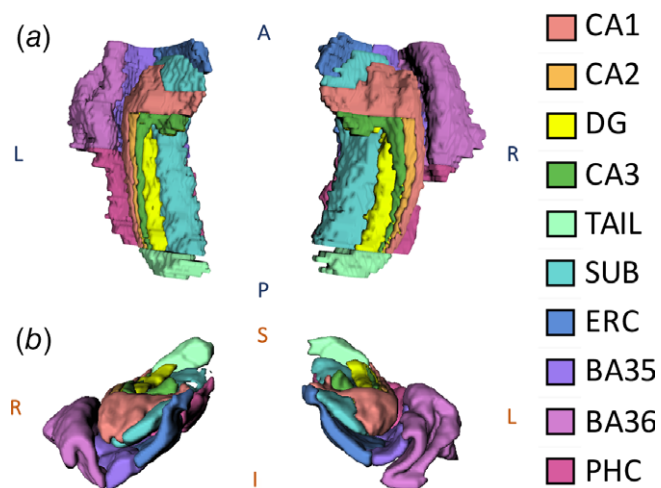


FIGURE 1 MTL segmentation from randomly chosen healthy adult rendered in 3D: (a) superior and (b) anterior 3D views. DG = dentate gyrus, SUB = subiculum, ERC = entorhinal cortex, BA35 + BA36 = Brodmann areas 35 & 36 (perirhinal cortex), and PHC = parahippocampal cortex

applied EPI distortion correction using B_0 maps, six-parameter rigid body motion correction (Friston, Frith, Frackowiak, & Turner, 1995), coregistration and resampling of the fMRI data to the high-resolution

structural MRI space (Kang, Yund, Herron, & Woods, 2007), band-pass filtering to 0.008–0.08 Hz, linear regression to factor out effects of global, mean white matter and mean cerebrospinal fluid signals (Van Dijk et al., 2010), as well as 12-parameter motion regression (Power, Barnes, Snyder, Schlaggar, & Petersen, 2012; Van Dijk, Sabuncu, & Buckner, 2012). All subjects experienced minimal head motion (<1 mm translation and $<0.5^\circ$ rotation in any direction) at all times during acquisition. To construct functional connectivity matrices for each subject, we calculated the Pearson correlation coefficient between the average residual time-series signals for all pairs of MTL subregions (Zalesky, Fornito, & Bullmore, 2012). We subsequently thresholded these matrices to remove negative weights (Rubinov & Sporns, 2010) and applied a Fisher r -z transform for variance stabilization (Fisher, 1921). In these networks, the MTL subregions served as network nodes, while the strength of correlation between subregions served as network edges.

Next, we computed three local network metrics that have proven particularly useful in describing important dimensions of variation in brain networks—connectivity strength (k_i), clustering coefficient (c_i), and efficiency (e_i)—largely due to their sensitivity to the markers of small-world architecture (Achard & Bullmore, 2007; Bassett & Bullmore, 2016; Bullmore & Sporns, 2009; Lynall et al., 2010; Onnela, Saramäki, Kertész, & Kaski, 2005; van den Heuvel & Sporns, 2013).

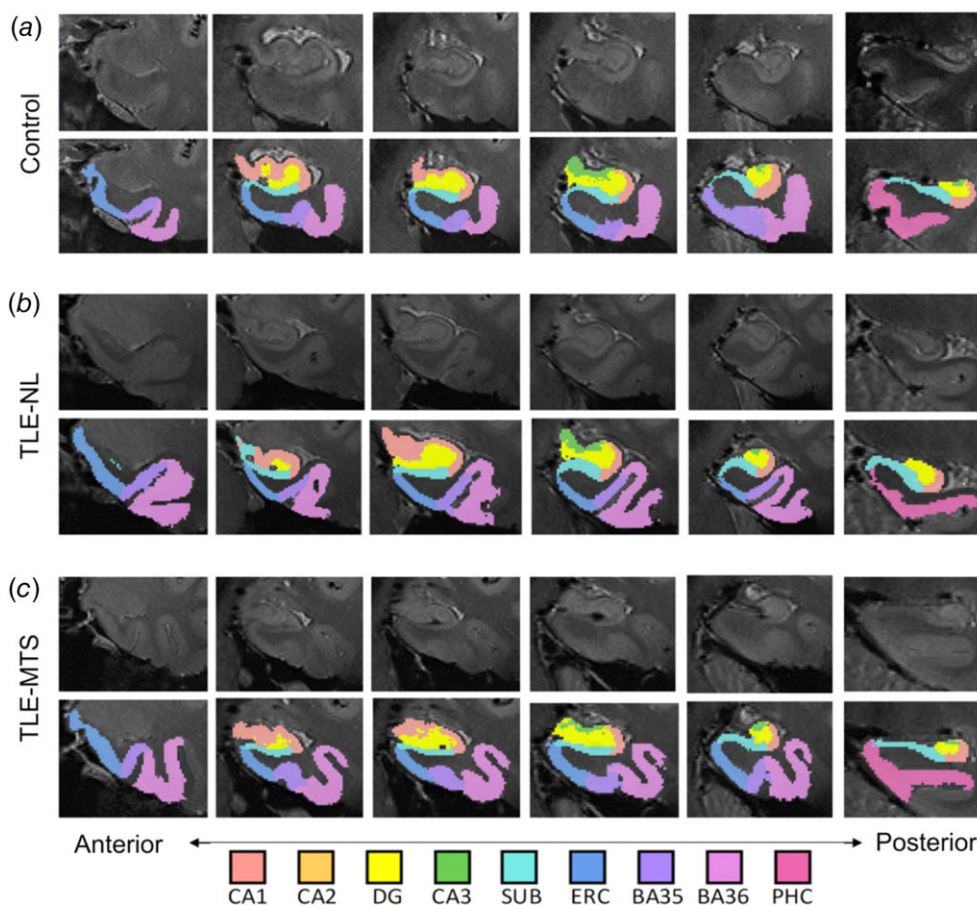


FIGURE 2 T2-weighted MRI coronal slices and corresponding automated segmentations overlaid onto left MTL in a representative (a) healthy control subject, (b) left-sided TLE-NL subject, and (c) left-sided TLE-MTS subject. High-resolution 7T MRI reveals grossly normal MTL architecture in controls and TLE-NL patients including clearly visible hippocampal digitations, and distortion of hippocampal architecture in TLE-MTS

Moreover, these metrics represent different ways of measuring any given node's level of centrality, or "hubness," within the network. Although there is no one agreed upon definition of a network hub (Zuo et al., 2012), it has been suggested that aggregating multiple network metrics can robustly characterize node hubness (van den Heuvel & Sporns, 2013). Modifying our previously described global network asymmetry metric (Shah et al., 2017) to allow for subregion-level analysis and to account for directionality in asymmetry, we defined a lateralized functional network asymmetry index, l_i , as the mean of the asymmetry indices for each subregion i across the three chosen network metrics. Formally,

$$l_{(i)} = \frac{1}{3} \left[\left(\frac{k_{i+N/2} - k_i}{k_{i+N/2} + k_i} \right) + \left(\frac{C_{i+N/2} - C_i}{C_{i+N/2} + C_i} \right) + \left(\frac{e_{i+N/2} - e_i}{e_{i+N/2} + e_i} \right) \right], \quad (1)$$

where the first $N/2$ nodes correspond to the MTL subregions contralateral to seizure onset and the last $N/2$ nodes correspond to the analogous MTL subregions ipsilateral to seizure onset. Like a standard asymmetry index, l_i can range from -1 to 1 . Intuitively, the variable l_i served as a simple summary metric of local intra-MTL functional network asymmetry. In addition to computing this summary metric of functional network asymmetry, we also computed subregional asymmetries for each individual functional network metric (strength, clustering coefficient, and local efficiency) to ensure robustness of our findings.

To assess network asymmetry across the entire hippocampus, we also computed the hippocampal functional network asymmetry as the weighted average of l_i over all subregions in the hippocampus proper (CA1, CA2, CA3, and DG), weighed by each region's bilateral volume. As in the volumetric asymmetry analysis, we normalized these indices via a z-score transformation with respect to the corresponding distribution of asymmetries in healthy controls.

2.6 | Statistical analysis

Statistical analyses were performed using nonparametric permutation-based tests (10,000 iterations) to avoid assumptions about the underlying distributions of the data. Analyses were performed separately for each asymmetry modality (volumetric and functional) and were applied to the z-transformed asymmetry indices which were normalized to the healthy control group. To characterize the difference in MTL subregional asymmetry between TLE-MTS and TLE-NL, we performed two-sample, two-tailed permutation tests for each subregion, using difference in group means as the test statistic. Additionally, within the regions for which there was a difference between TLE-MTS and TLE-NL, we performed one-sample two-tailed permutation tests to determine if the subregional asymmetries were significantly different from zero.

2.7 | Software

Image processing, network analyses, and statistical analyses were implemented using SPM (Friston et al., 1994), FSL (Smith et al., 2004), ANTs (Avants et al., 2011), the Brain Connectivity Toolbox (Rubinov & Sporns, 2010), and custom python scripts available publicly at <https://github.com/shahpreya/MTLnet>.

3 | RESULTS

3.1 | MTL volumetric asymmetry

At the group level, we observed significant differences in volumetric asymmetries between TLE-MTS and TLE-NL in CA1, CA2, CA3, DG, and subiculum, as well as the whole hippocampus ($p < .05$, two-tailed two-sample permutation test) (Figure 3(a), Supporting Information Table 1). Laterality analysis indicated that there was significant positive asymmetry (contralateral volume $>$ ipsilateral volume) within all of these regions in TLE-MTS and within the whole hippocampus in TLE-NL (two-tailed one-sample permutation test) (Figure 3(a)).

At the individual patient level, we found that four of four TLE-MTS patients presented with positive volumetric asymmetries (contralateral $>$ ipsilateral) in all hippocampal subfields (CA1, CA2, CA3, and DG), subiculum, and BA35; three of those four patients also had positive volumetric asymmetries in the entorhinal cortex. The patterns of subregional asymmetry in individual TLE-NL patients were much more heterogeneous, with only two of nine patients exhibiting positive asymmetries (contralateral $>$ ipsilateral) across all hippocampal subfields, though seven of nine patients exhibited whole-hippocampal positive asymmetry. Subject-level volumetric asymmetry heat maps (Supporting Information Figure S1a) and group-averaged volumetric asymmetries mapped onto MTL segmentations (Figure 3(b)) illustrate these patterns.

3.2 | MTL functional network asymmetry

At the group level, we found significant differences in functional network asymmetries between TLE-MTS and TLE-NL in CA1 and the whole hippocampus ($p < .05$, two-tailed two-sample permutation test) (Figure 4(a), Supporting Information Table S1). The directionality and significance of this finding persisted using the metrics of strength asymmetry, clustering coefficient asymmetry, and local efficiency asymmetry (Supporting Information Figure S2). Laterality analysis indicated that within the CA1 and the whole hippocampus, there was significant positive asymmetry (contralateral $>$ ipsilateral) in TLE-MTS and significant negative asymmetry (ipsilateral $>$ contralateral) in TLE-NL ($p < .05$, two-tailed one-sample permutation test) (Figure 4(a)). The directionality and trends of these findings also persisted using the metrics of strength asymmetry, clustering coefficient asymmetry, and local efficiency asymmetry (Supporting Information Figure S2).

At the individual patient level, we found that four of four TLE-MTS patients presented with positive functional network asymmetry values (contralateral $>$ ipsilateral) in the CA1 and BA35 subregions, whereas patterns of functional network asymmetry in the remaining MTL subregions were heterogeneous. In contrast, we found that eight of nine TLE-NL patients exhibited negative functional network asymmetry values (ipsilateral $>$ contralateral) in the whole hippocampus, with the majority of TLE-NL patients also having negative functional network asymmetry in individual subfields CA1 (7/9), CA2 (8/9), CA3 (8/9), and DG (7/9). Subject-level functional asymmetry heat maps (Supporting Information Figure S1b) and group-averaged functional network asymmetries mapped onto MTL segmentations (Figure 4(b)) illustrate these patterns.

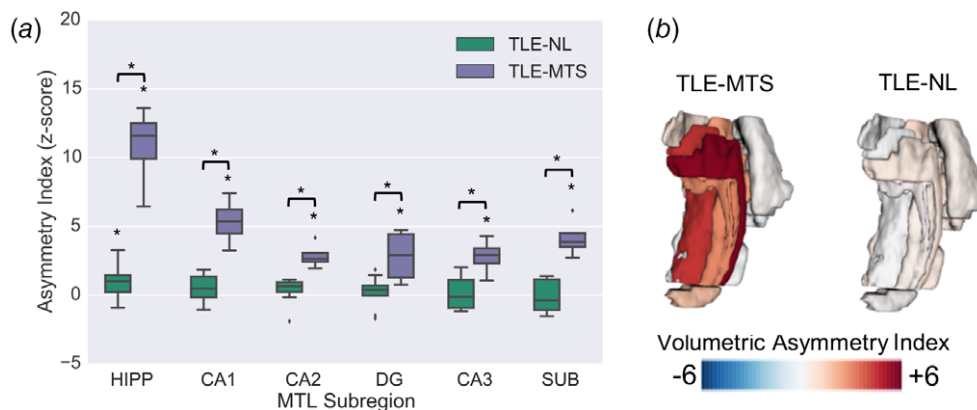


FIGURE 3 MTL volumetric asymmetry analyses. (a) Normalized volumetric asymmetries in TLE-NL and TLE-MTS patients ($*p < .05$) in hippocampal ROIs. (b) Visualization of mean volumetric asymmetries overlaid onto MTL segmentation for each TLE group

4 | DISCUSSION

The goal of this study was to develop an approach to explore MTL subregional asymmetry-based metrics in TLE, and characterize differences between TLE-NL and TLE-MTS. First, we performed automated segmentation of MTL subregions on 7T MRI data from TLE-MTS and TLE-NL patients as well as healthy controls. Next, we computed subregional volumetric asymmetries from T2-weighted MRI and functional network asymmetries from resting-state BOLD-fMRI. We found that patterns of volumetric and functional asymmetry were different between the two TLE subtypes. Notably, we found distinct patterns of functional asymmetry in the CA1 subfield and whole hippocampus, with TLE-NL patients exhibiting negative (ipsilateral > contralateral) functional network asymmetry, and TLE-MTS patients exhibiting positive (contralateral > ipsilateral) functional network asymmetry.

4.1 | Asymmetry-based findings

We found that TLE-MTS patients exhibited positive volumetric asymmetry (i.e., contralateral volume was greater than ipsilateral) in the whole hippocampus and multiple hippocampal subfields. These findings are consistent with our knowledge that MTS is associated with histological patterns of neuronal loss and gliosis which can be

limited to Ammon's horn (CA subfields of the hippocampus) or extend to the DG and extra-hippocampal MTL subregions (Thom, 2014; Wieser, 2004). Additionally, our findings corroborate a hippocampal subfield neuroimaging study at 4T that revealed ipsilateral atrophy in CA1, CA2, and combined CA3&DG subfields in TLE-MTS, but did not reveal significant atrophy in TLE-NL (Mueller et al., 2009). Our findings are also consistent with another recent study at 3T that revealed volume reduction in multiple hippocampal subfields in TLE-MTS but not TLE-NL (Sone et al., 2016). Consistency with prior studies validates our approach of applying automated segmentation algorithms to 7T structural MRI to characterize expected patterns of asymmetry in TLE-MTS.

We also observed that TLE-MTS patients exhibited statistically significant positive functional network asymmetry in the CA1 subregion. This observation corroborates prior resting-state fMRI findings of reduced ipsilateral functional connectivity within the MTL in TLE studies in which all (Pereira et al., 2010) or most (Bettus et al., 2008; Bettus et al., 2010) patients had MTS. In contrast, TLE-NL patients exhibited significant negative functional network asymmetry (i.e., ipsilateral connectivity was greater than contralateral) in the whole hippocampus and in CA1, and this trend was present for all hippocampal subfields. Although further work is necessary to provide a mechanistic explanation for this observation, studies using intracranial recordings indicate that epilepsy is characterized by increased

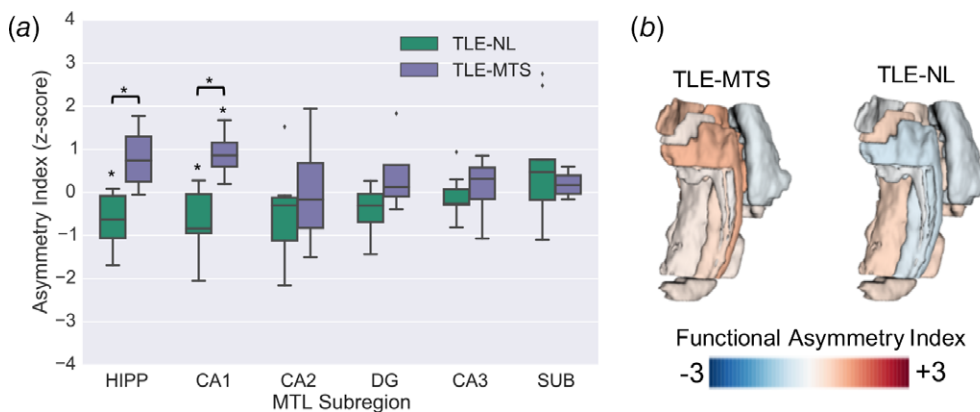


FIGURE 4 MTL functional asymmetry analyses. (a) Normalized functional asymmetries in TLE-NL and TLE-MTS patients ($*p < .05$) in hippocampal ROIs. (b) Visualization of mean functional asymmetries overlaid onto MTL segmentation for each TLE group

synchronization in the epileptic zone both ictally (Bartolomei et al., 2004; Bragin, Engel, Wilson, Fried, & Buzsáki, 1999; Engel, 2001; Uhlhaas & Singer, 2006) and interictally (Bettus et al., 2008; Schevon et al., 2007). Therefore, an increase in ipsilateral functional network connectivity relative to the contralateral side could indicate greater synchronization of the seizure onset region with the remaining MTL network, even during the interictal state. The localization of functional network asymmetry to CA1, along with our previous finding that CA1 is a functional hub within the MTL network (Shah et al., 2018), support the hypothesis that CA1 is a key player in the TLE-NL network and could be a target for ablation or stimulation.

The different patterns of asymmetry in TLE-MTS and TLE-NL indicate that these two TLE subtypes have distinct phenotypes. Our findings add to a growing body of literature suggesting that MRI-negative TLE may have a different pathophysiology than TLE-MTS and is not simply an early variant (Bernhardt et al., 2016a; Liu et al., 2012; Muhlhof et al., 2017; Reyes et al., 2016; Vaughan et al., 2016). These differences suggest that future studies would do well to separate these subtypes in group-level analyses to further characterize their differences and avoid confounding effects.

4.2 | Methodological considerations and limitations

Our findings in TLE-MTS patients should be interpreted with caveats. First, since MTS is associated with loss of normal internal hippocampal architecture due to neuronal cell loss and gliosis (Elkommos et al., 2016; Jackson, Berkovic, Duncan, & Connelly, 1993), as well as hyperintensity on T2-weighted images (Engel, 2001; Kuzniecky & Jackson, 2005), segmentation boundaries in TLE-MTS patients are inherently less reliable than in subjects with normal MTLs. These observations suggest that the volumes computed from these patients have an intrinsically higher degree of uncertainty. A related consequence is that segmented subregions include gliotic and sclerotic tissue, which may be functionally inactive. Such altered tissue functionality could explain decreased ipsilateral functional hippocampal connectivity in MTS patients. Since the presence of distorted MTL architecture is a fundamental property of MTS, it cannot be avoided. However, we did visually inspect all subjects' segmentations to confirm that they were consistent with our knowledge of MTL architecture. Moreover, since our segmentations are automated, they are free from human bias.

It is important to note that the differences in functional connectivity between TLE groups and controls were subtle, and that our sample size was modest. Therefore, our findings should be corroborated on larger data sets across multiple institutions, scanners, and protocols. We also note that there is considerable heterogeneity inherent to epilepsy patient data, including potential confounding factors such as duration of epilepsy, number of drug trials, cause of epilepsy, laterality, etiology, and seizure frequency. Although we attempted to minimize confounds by limiting our data set to subjects with clearly defined mesial temporal origin and no extra-mesial abnormalities, we emphasize that our study is exploratory. Nonetheless, our approach paves the way for future studies in larger cohorts and in combination with other modalities. Additionally, our methodology can be applied to other disorders in which hippocampal asymmetry has been implicated, such as schizophrenia (Fukuzako et al., 1997), Alzheimer's disease (Shi, Liu, Zhou, Yu, & Jiang, 2009), and semantic dementia (La Joie et al., 2013).

4.3 | Conclusions

This study presents preliminary data characterizing intra-MTL structural and functional asymmetry in TLE and has important implications for our understanding of MTL topology in both normal and pathological human brains. We hope these results will encourage further research on the utility of MTL subregional asymmetry features for precise localization of abnormalities in TLE, allowing for more targeted therapies. Although further validation in larger data sets is needed along with comparison to other modalities, our study highlights the promise of combining high-resolution imaging, automated segmentation techniques, and network analytical approaches in order to uncover brain network abnormalities that were previously invisible.

ACKNOWLEDGMENTS

This work was supported by National Institutes of Health grants T32-EB009384, R03-EB16923-01A1, K23-NS073801-01, 1R01NS099348-02, R01NS085211, R01MH112847, and R01EB017255. We also acknowledge support from the Transdisciplinary Awards Program in Translational Medicine and Therapeutics-Translational Biomedical Imaging Core (TAPITMAT-TBIC) under UL1TR001878, the Center for Biomedical Image Computing and Analytics Seed Award, the Mirowski Family Foundation, and the Thornton Foundation.

DECLARATIONS OF INTEREST

None.

ORCID

Preya Shah  <https://orcid.org/0000-0001-8360-6400>

Danielle S. Bassett  <https://orcid.org/0000-0002-6183-4493>

Kathryn A. Davis  <https://orcid.org/0000-0002-7020-6480>

REFERENCES

- Achard, S., & Bullmore, E. (2007). Efficiency and cost of economical brain functional networks. *PLoS Computational Biology*, 3(2), 0174–0183. <https://doi.org/10.1371/journal.pcbi.0030017>
- Avants, B. B., Tustison, N. J., Song, G., Cook, P. A., Klein, A., & Gee, J. C. (2011). A reproducible evaluation of ANTs similarity metric performance in brain image registration. *Neuroimage*, 54, 2033–2044. <http://www.ncbi.nlm.nih.gov/pubmed/20851191>
- Balchandani, P., & Naidich, T. P. (2015). Ultra-high-field MR neuroimaging. *American Journal of Neuroradiology*, 36, 1204–1215. <https://doi.org/10.3174/ajnr.A4180>
- Barron, D. S., Fox, P. T., Pardoe, H., Lancaster, J., Price, L. R., Blackmon, K., ... Thesen, T. (2015). Thalamic functional connectivity predicts seizure laterality in individual TLE patients: Application of a biomarker development strategy. *NeuroImage Clinical*, 7, 273–280. <https://doi.org/10.1016/j.nicl.2014.08.002>
- Bartolomei, F., Wendling, F., Régis, J., Gavaret, M., Guye, M., & Chauvel, P. (2004). Pre-ictal synchronicity in limbic networks of mesial temporal lobe epilepsy. *Epilepsy Research*, 61(61), 89–104. <https://doi.org/10.1016/j.eplepsyres.2004.06.006>
- Bassett, D. S., & Bullmore, E. T. (2016). Small-world brain networks revisited. *The Neuroscientist*, 23(5), 499–516. <https://doi.org/10.1177/1073858416667720>
- Bernhardt, B. C., Bernasconi, A., Liu, M., Hong, S.-J., Caldarou, B., Goubran, M., ... Bernasconi, N. (2016). The spectrum of structural and functional imaging abnormalities in temporal lobe epilepsy. *Annals of Neurology*, 80(1), 142–153. <https://doi.org/10.1002/ana.24691>

- Bernhardt, B. C., Hong, S., Bernasconi, A., & Bernasconi, N. (2013). Imaging structural and functional brain networks in temporal lobe epilepsy. *Frontiers in Human Neuroscience*, 7, 624. <https://doi.org/10.3389/fnhum.2013.00624>
- Bettus, G., Bartolomei, F., Confort-Gouny, S., Guedj, E., Chauvel, P., Cozzone, P. J., ... Guye, M. (2010). Role of resting state functional connectivity MRI in presurgical investigation of mesial temporal lobe epilepsy. *Journal of Neurology, Neurosurgery, and Psychiatry*, 81(10), 1147–1154. <https://doi.org/10.1136/jnnp.2009.191460>
- Bettus, G., Guedj, E., Joyeux, F., Confort-Gouny, S., Soulier, E., Laguitton, V., ... Guye, M. (2008). Decreased basal fMRI functional connectivity in epileptogenic networks and contralateral compensatory mechanisms. *Human Brain Mapping*, 30, 1580–1591.
- Bettus, G., Wendling, F., Guye, M., Valton, L., Régis, J., Chauvel, P., & Bartolomei, F. (2008). Enhanced EEG functional connectivity in mesial temporal lobe epilepsy. *Epilepsy Research*, 81(1), 58–68. <https://doi.org/10.1016/j.eplepsyres.2008.04.020>
- Blümcke, I., Thom, M., Aronica, E., Armstrong, D. D., Bartolomei, F., Bernasconi, A., ... Spreafico, R. (2013). International consensus classification of hippocampal sclerosis in temporal lobe epilepsy: A task force report from the ILAE commission on diagnostic methods. *Epilepsia*, 54(7), 1315–1329. <https://doi.org/10.1111/epi.12220>
- Bonilha, L., Martz, G. U., Glazier, S. S., & Edwards, J. C. (2012, January). Subtypes of medial temporal lobe epilepsy: Influence on temporal lobectomy outcomes? *Epilepsia*, 53(1), 1–6. <https://doi.org/10.1111/j.1528-1167.2011.03298.x>
- Bragin, A., Engel, J., Wilson, C. L., Fried, I., & Buzsáki, G. (1999). High-frequency oscillations in human brain. *Hippocampus*, 9(2), 137–142. [https://doi.org/10.1002/\(SICI\)1098-1063\(1999\)9:2<137::AID-HIPO5>3.0.CO;2-0](https://doi.org/10.1002/(SICI)1098-1063(1999)9:2<137::AID-HIPO5>3.0.CO;2-0)
- Bullmore, E., & Sporns, O. (2009). Complex brain networks: Graph theoretical analysis of structural and functional systems. *Nature Reviews Neuroscience*, 10(3), 186–198. <https://doi.org/10.1038/nrn2575>
- Chiang, S., & Haneef, Z. (2014). Graph theory findings in the pathophysiology of temporal lobe epilepsy. *Clinical Neurophysiology*, 125(7), 1295–1305. <https://doi.org/10.1016/j.clinph.2014.04.004>
- Chu, C. J., Kramer, M. A., Pathmanathan, J., Bianchi, M. T., Westover, M. B., Wison, L., & Cash, S. S. (2012). Emergence of stable functional networks in long-term human electroencephalography. *Journal of Neuroscience*, 32(8), 2703–2713. <https://doi.org/10.1523/JNEUROSCI.5669-11.2012>
- Cook, M. J., Fish, D. R., Shorvon, S. D., Straughan, K., & Stevens, J. M. (1992). Hippocampal volumetric and morphometric studies in frontal and temporal lobe epilepsy. *Brain*, 115(Pt 4), 1001–1015.
- Davis, K. A., Nanga, R. P. R., Das, S., Chen, S. H., Hadar, P. N., Pollard, J. R., ... Reddy, R. (2015). Glutamate imaging (GluCEST) lateralizes epileptic foci in nonlesional temporal lobe epilepsy. *Science Translational Medicine*, 7(309), 309ra161. <https://doi.org/10.1126/scitranslmed.aaa7095>
- Elkommos, S., Weber, B., Niehusmann, P., Volmering, E., Richardson, M. P., Goh, Y. Y., ... Keller, S. S. (2016). Hippocampal internal architecture and postoperative seizure outcome in temporal lobe epilepsy due to hippocampal sclerosis. *Seizure*, 35, 65–71. <https://doi.org/10.1016/j.seizure.2016.01.007>
- Engel, J. (1996). Surgery for seizures. *New England Journal of Medicine*, 334(10), 647–653. <https://doi.org/10.1056/NEJM199603073341008>
- Engel, J. (2001). Mesial temporal lobe epilepsy: What have we learned? *The Neuroscientist*, 7(4), 340–352. <https://doi.org/10.1177/107385840100700410>
- Farid, N., Girard, H. M., Kemmotsu, N., Smith, M. E., Magda, S. W., Lim, W. Y., ... McDonald, C. R. (2012). Temporal lobe epilepsy: Quantitative MR volumetry in detection of hippocampal atrophy. *Radiology*, 264(2), 542–550. <https://doi.org/10.1148/radiol.12112638>
- Fisher, R. A. (1921). On the “probable error” of a coefficient of correlation deduced from a small sample. *Metron*, 1, 3–32. <https://doi.org/10.2307/1928524>
- Fisher, R. S., & Velasco, A. L. (2014). Electrical brain stimulation for epilepsy. *Nature Reviews Neurology*, 10(5), 261–270. <https://doi.org/10.1038/nrneuro.2014.59>
- Friston, K. J., Frith, C. D., Frackowiak, R. S., & Turner, R. (1995). Characterizing dynamic brain responses with fMRI: A multivariate approach. *NeuroImage*, 2(2), 166–172.
- Friston, K. J., Holmes, A. P., Worsley, K. J., Poline, J. P., Frith, C. D., & Frackowiak, R. S. J. (1994). Statistical parametric maps in functional imaging: A general linear approach. *Human Brain Mapping*, 2(4), 189–210. <https://doi.org/10.1002/hbm.460020402>
- Fukuzako, H., Yamada, K., Kodama, S., Yonezawa, T., Fukuzako, T., Takenouchi, K., ... Takigawa, M. (1997). Hippocampal volume asymmetry and age at illness onset in males with schizophrenia. *European Archives of Psychiatry and Clinical Neuroscience*, 247(5), 248–251.
- Goffin, K., Van Paesschen, W., Dupont, P., Baete, K., Palmieri, A., Nuyts, J., & Van Laere, K. (2010). Anatomy-based reconstruction of FDG-PET images with implicit partial volume correction improves detection of hypometabolic regions in patients with epilepsy due to focal cortical dysplasia diagnosed on MRI. *European Journal of Nuclear Medicine and Molecular Imaging*, 37(6), 1148–1155. <https://doi.org/10.1007/s00259-010-1405-5>
- Haneef, Z., & Chiang, S. (2014). Clinical correlates of graph theory findings in temporal lobe epilepsy. *Seizure*, 23(10), 809–818. <https://doi.org/10.1016/j.seizure.2014.07.004>
- Haneef, Z., Lenartowicz, A., Yeh, H. J., Engel, J., & Stern, J. M. (2014). Network analysis of the default mode network using functional connectivity MRI in temporal lobe epilepsy. *Journal of Visualized Experiments*, 90, e51442. <https://doi.org/10.3791/51442>
- He, X., Doucet, G. E., Sperling, M., Sharan, A., & Tracy, J. I. (2015). Reduced thalamocortical functional connectivity in temporal lobe epilepsy. *Epilepsia*, 56(10), 1571–1579. <https://doi.org/10.1111/epi.13085>
- Henry, T. R., Chupin, M., Lehericy, S., Strupp, J. P., Sikora, M. A., Sha, Z. Y., ... Van de Moortele, P. F. (2011). Hippocampal sclerosis in temporal lobe epilepsy: Findings at 7 T(1). *Radiology*, 261(1), 199–209. <http://doi.org/radiol.11101651>
- Jackson, G. D., Berkovic, S. F., Duncan, J. S., & Connelly, A. (1993). Optimizing the diagnosis of hippocampal sclerosis using MR imaging. *American Journal of Neuroradiology*, 14(3), 753–762.
- James, G. A., Tripathi, S. P., Ojemann, J. G., Gross, R. E., & Drane, D. L. (2013). Diminished default mode network recruitment of the hippocampus and parahippocampus in temporal lobe epilepsy. *Journal of Neurosurgery*, 119(2), 288–300. <https://doi.org/10.3171/2013.JNS121041>
- Jokeit, H., Okujava, M., & Woermann, F. G. (2001). Memory fMRI lateralizes temporal lobe epilepsy. *Neurology*, 57(10), 1786–1793. <https://doi.org/10.1212/WNL.57.10.1786>
- Kang, X., Yund, E. W., Herron, T. J., & Woods, D. L. (2007). Improving the resolution of functional brain imaging: Analyzing functional data in anatomical space. *Magnetic Resonance Imaging*, 25(7), 1070–1078. <https://doi.org/10.1016/j.mri.2006.12.005>
- Khambhati, A. N., Davis, K. A., Lucas, T. H., Litt, B., & Bassett, D. S. (2016). Virtual cortical resection reveals push-pull network control preceding seizure evolution. *Neuron*, 91(5), 1170–1182. <https://doi.org/10.1016/j.neuron.2016.07.039>
- Kuzniecky, R. I., & Jackson, G. D. (2005). *Magnetic resonance in epilepsy*. Academic Press. <https://doi.org/10.1016/B978-0-12-431152-7.X5000-9>
- Kwan, P., Schachter, S. C., & Brodie, M. J. (2011). Drug-resistant epilepsy. *The New England Journal of Medicine*, 365(8), 919–926.
- La Joie, R., Perrotin, A., De La Sayette, V., Egret, S., Dœuvre, L., Belliard, S., ... Chételat, G. (2013). Hippocampal subfield volumetry in mild cognitive impairment, Alzheimer's disease and semantic dementia. *NeuroImage Clinical*, 3, 155–162. <https://doi.org/10.1016/j.nicl.2013.08.007>
- Li, Y.-J., Ga, S.-N., Huo, Y., Li, S.-Y., & Gao, X.-G. (2007). Characteristics of hippocampal volumes in healthy Chinese from MRI. *Neurological Research*, 29(8), 803–806. <https://doi.org/10.1179/O16164107X223557>
- Liao, W., Zhang, Z., Pan, Z., Mantini, D., Ding, J., Duan, X., ... Chen, H. (2010). Altered functional connectivity and small-world in mesial temporal lobe epilepsy. *PLoS One*, 5(1), e8525. <https://doi.org/10.1371/journal.pone.0008525>
- Liu, M., Concha, L., Lebel, C., Beaulieu, C., & Gross, D. W. (2012). Mesial temporal sclerosis is linked with more widespread white matter changes in temporal lobe epilepsy. *NeuroImage Clinical*, 1(1), 99–105. <https://doi.org/10.1016/j.nicl.2012.09.010>
- Lynall, M.-E., Bassett, D. S., Kerwin, R., McKenna, P. J., Kitzbichler, M., Muller, U., & Bullmore, E. (2010). Functional connectivity and brain

- networks in schizophrenia. *Journal of Neuroscience*, 30(28), 9477–9487. <https://doi.org/10.1523/JNEUROSCI.0333-10.2010>
- Morgan, V. L., Sonmez Turk, H. H., Gore, J. C., & Abou-Khalil, B. (2012). Lateralization of temporal lobe epilepsy using resting functional magnetic resonance imaging connectivity of hippocampal networks. *Epilepsia*, 53(9), 1628–1635. <https://doi.org/10.1111/j.1528-1167.2012.03590.x>
- Mueller, S. G., Laxer, K. D., Barakos, J., Cheong, I., Garcia, P., & Weiner, M. W. (2009). Subfield atrophy pattern in temporal lobe epilepsy with and without mesial sclerosis detected by high-resolution MRI at 4 tesla: Preliminary results. *Epilepsia*, 50(6), 1474–1483. <https://doi.org/10.1111/j.1528-1167.2009.02010.x>
- Muhlhofer, W., Tan, Y.-L., Mueller, S. G., & Knowlton, R. (2017). MRI-negative temporal lobe epilepsy—what do we know? *Epilepsia*, 58(5), 727–742. <https://doi.org/10.1111/epi.13699>
- Onnela, J. P., Saramäki, J., Kertész, J., & Kaski, K. (2005). Intensity and coherence of motifs in weighted complex networks. *Physical Review E - Statistical, Nonlinear, and Soft Matter Physics*, 71(6), 065103. <https://doi.org/10.1103/PhysRevE.71.065103>
- Oppenheim, C., Dormont, D., Biondi, A., Lehericy, S., Hasboun, D., Clémenceau, S., ... Marsault, C. (1998). Loss of digitations of the hippocampal head on high-resolution fast spin-echo MR: A sign of mesial temporal sclerosis. *American Journal of Neuroradiology*, 19(3), 457–463.
- Pereira, F. R., Alessio, A., Sercheli, M. S., Pedro, T., Bilevicius, E., Rondina, J. M., ... Cendes, F. (2010). Asymmetrical hippocampal connectivity in mesial temporal lobe epilepsy: Evidence from resting state fMRI. *BMC Neuroscience*, 11(1), 66. <https://doi.org/10.1186/1471-2202-11-66>
- Pittau, F., Grova, C., Moeller, F., Dubeau, F., & Gotman, J. (2012). Patterns of altered functional connectivity in mesial temporal lobe epilepsy. *Epilepsia*, 53(6), 1013–1023. <https://doi.org/10.1111/j.1528-1167.2012.03464.x>
- Power, J. D., Barnes, K. A., Snyder, A. Z., Schlaggar, B. L., & Petersen, S. E. (2012). Spurious but systematic correlations in functional connectivity MRI networks arise from subject motion. *NeuroImage*, 59(3), 2142–2154. <https://doi.org/10.1016/j.neuroimage.2011.10.018>
- Reyes, A., Thesen, T., Wang, X., Hahn, D., Yoo, D., Kuzniecky, R., ... Blackmon, K. (2016). Resting-state functional MRI distinguishes temporal lobe epilepsy subtypes. *Epilepsia*, 57(9), 1475–1484. <https://doi.org/10.1111/epi.13456>
- Rubinov, M., & Sporns, O. (2010). Complex network measures of brain connectivity: Uses and interpretations. *NeuroImage*, 52(3), 1059–1069. <https://doi.org/10.1016/j.neuroimage.2009.10.003>
- Schevon, C. A., Cappell, J., Emerson, R., Isler, J., Grieve, P., Goodman, R., ... Gilliam, F. (2007). Cortical abnormalities in epilepsy revealed by local EEG synchrony. *NeuroImage*, 35(1), 140–148. <https://doi.org/10.1016/j.neuroimage.2006.11.009>
- Shah, P., Bassett, D. S., Wisse, L. E. M., Detre, J. A., Stein, J. M., Yushkevich, P. A., ... Das, S. R. (2018). Mapping the structural and functional network architecture of the medial temporal lobe using 7T MRI. *Human Brain Mapping*, 39(2), 851–865. <https://doi.org/10.1002/hbm.23887>
- Sharma, A. K., Reams, R. Y., Jordan, W. H., Miller, M. A., Thacker, H. L., & Snyder, P. W. (2007). Mesial temporal lobe epilepsy: pathogenesis, induced rodent models and lesions. *Toxicologic Pathology*, 35(7), 984–999. <https://doi.org/10.1080/01926230701748305>
- Shi, F., Liu, B., Zhou, Y., Yu, C., & Jiang, T. (2009). Hippocampal volume and asymmetry in mild cognitive impairment and Alzheimer's disease: Meta-analyses of MRI studies. *Hippocampus*, 19(11), 1055–1064. <https://doi.org/10.1002/hipo.20573>
- Siegel, A. M., Jobst, B. C., Thadani, V. M., Rhodes, C. H., Lewis, P. J., Roberts, D. W., & Williamson, P. D. (2001). Medically intractable, localization-related epilepsy with normal MRI: presurgical evaluation and surgical outcome in 43 patients. *Epilepsia*, 42(7), 883–888. <https://doi.org/10.1046/j.1528-1157.2001.042007883.x>
- Smith, S. M., Jenkinson, M., Woolrich, M. W., Beckmann, C. F., Behrens, T. E. J., Johansen-Berg, H., ... Matthews, P. M. (2004). Advances in functional and structural MR image analysis and implementation as FSL. *NeuroImage*, 23, S208–S219. <https://doi.org/10.1016/j.neuroimage.2004.07.051>
- Sone, D., Sato, N., Maikusa, N., Ota, M., Sumida, K., Yokoyama, K., ... Matsuda, H. (2016). Automated subfield volumetric analysis of hippocampus in temporal lobe epilepsy using high-resolution T2-weighted MR imaging. *NeuroImage Clinical*, 12, 57–64. <https://doi.org/10.1016/j.nicl.2016.06.008>
- Télez-Zenteno, J. F., Ronquillo, L. H., Moien-Afshari, F., & Wiebe, S. (2010). Surgical outcomes in lesional and non-lesional epilepsy: A systematic review and meta-analysis. *Epilepsy Research*, 89(2–3), 310–318. <https://doi.org/10.1016/j.eplepsyres.2010.02.007>
- Thom, M. (2014). Review: Hippocampal sclerosis in epilepsy: A neuropathology review. *Neuropathology and Applied Neurobiology*, 40(5), 520–543. <https://doi.org/10.1111/nan.12150>
- Uhlhaas, P. J., & Singer, W. (2006). Neural synchrony in brain disorders: Relevance for cognitive dysfunctions and pathophysiology. *Neuron*, 52(1), 155–168. <https://doi.org/10.1016/j.neuron.2006.09.020>
- van den Heuvel, M. P., & Sporns, O. (2013). Network hubs in the human brain. *Trends in Cognitive Sciences*, 17(12), 683–696. <https://doi.org/10.1016/j.tics.2013.09.012>
- van der Kolk, A. G., Hendrikse, J., Zwanenburg, J. J. M., Visser, F., & Luijten, P. R. (2013). Clinical applications of 7T MRI in the brain. *European Journal of Radiology*, 82(5), 708–718. <https://doi.org/10.1016/j.ejrad.2011.07.007>
- Van Dijk, K. R. A., Hedden, T., Venkataraman, A., Evans, K. C., Lazar, S. W., & Buckner, R. L. (2010). Intrinsic functional connectivity as a tool for human connectomics: Theory, properties, and optimization. *Journal of Neurophysiology*, 103(1), 297–321.
- Van Dijk, K. R. A., Sabuncu, M. R., & Buckner, R. L. (2012). The influence of head motion on intrinsic functional connectivity MRI. *NeuroImage*, 59(1), 431–438. <https://doi.org/10.1016/j.neuroimage.2011.07.044>
- Vaughan, D. N., Rayner, G., Tailby, C., & Jackson, G. D. (2016). MRI-negative temporal lobe epilepsy. *Neurology*, 87(18), 1934–1942. <https://doi.org/10.1212/WNL.0000000000003289>
- Ver Hoef, L. W., Paige, A. L., Riley, K. O., Cure, J., Soltani, M., Williams, F. B., ... Knowlton, R. C. (2013). Evaluating hippocampal internal architecture on MRI: Inter-rater reliability of a proposed scoring system. *Epilepsy Research*, 106(1–2), 146–154. <https://doi.org/10.1016/j.eplepsyres.2013.05.009>
- Ver Hoef, L. W., Williams, F. B., Kennedy, R. E., Szafarski, J. P., & Knowlton, R. C. (2013). Predictive value of hippocampal internal architecture asymmetry in temporal lobe epilepsy. *Epilepsy Research*, 106(1–2), 155–163. <https://doi.org/10.1016/j.eplepsyres.2013.05.008>
- Wennberg, R., Arruda, F., Quesney, L. F., & Olivier, A. (2002). Preeminence of extrahippocampal structures in the generation of mesial temporal seizures: Evidence from human depth electrode recordings. *Epilepsia*, 43(7), 716–726.
- Wieser, H.-G. (2004). Mesial temporal lobe epilepsy with hippocampal sclerosis. *Epilepsia*, 45(6), 695–714. <https://doi.org/10.1111/j.0013-9580.2004.09004.x>
- Willie, J. T., Laxpati, N. G., Drane, D. L., Gowda, A., Appin, C., Hao, C., ... Gross, R. E. (2014). Real-time magnetic resonance-guided stereotactic laser amygdalohippocampotomy for mesial temporal lobe epilepsy. *Neurosurgery*, 74(6), 569–584. <https://doi.org/10.1227/NEU.0000000000000343>
- Yushkevich, P. A., Pluta, J. B., Wang, H., Xie, L., Ding, S.-L., Gertje, E. C., ... Wolk, D. A. (2015). Automated volumetry and regional thickness analysis of hippocampal subfields and medial temporal cortical structures in mild cognitive impairment. *Human Brain Mapping*, 36(1), 258–287. <https://doi.org/10.1002/hbm.22627>
- Zalesky, A., Fornito, A., & Bullmore, E. (2012). On the use of correlation as a measure of network connectivity. *NeuroImage*, 60(4), 2096–2106. <https://doi.org/10.1016/j.neuroimage.2012.02.001>

SUPPORTING INFORMATION

Additional supporting information may be found online in the Supporting Information section at the end of the article.

How to cite this article: Shah P, Bassett DS, Wisse LEM, et al. Structural and functional asymmetry of medial temporal subregions in unilateral temporal lobe epilepsy: A 7T MRI study. *Hum Brain Mapp*. 2019;40:2390–2398. <https://doi.org/10.1002/hbm.24530>